Supporting Information

Dynamic behavior of liquid droplets with enzyme compartmentalization triggered by sequential glycolytic enzyme reactions

Tomoto Ura,[†,§] Shunsuke Tomita,[§] and Kentaro Shiraki[†]

[†] Faculty of Pure and Applied Sciences, University of Tsukuba, 1-1-1 Tennodai, Tsukuba, Ibaraki 305-8573, Japan.

[§] Health and Medical Research Institute, National Institute of Advanced Industrial Science and Technology, 1-1-1 Higashi, Tsukuba, Ibaraki 305-8566, Japan.

Section 1. Experimental details

Materials

Adenosine 5'-triphosphate disodium salt hydrate (ATP) and adenosine 5'-diphosphate disodium salt hydrate (ADP) were obtained from Tokyo Chemical Industry co, Ltd. (Tokyo, Japan). 4-(2-Hydroxyethyl)-1-piperazineethanesulfonic acid (HEPES), β-nicotinamide adenine dinucleotide phosphate tetrasodium salt (Reduced Form) (NADPH), β-nicotinamide adenine dinucleotide phosphate sodium salt (NADP), β-nicotinamide adenine dinucleotide (NAD), and β-nicotinamide adenine dinucleotide disodium salt (reduced form) (NADH) were obtained from Nacalai Tesque (Kyoto, Japan). Magnesium chloride hexahydrate, D (+)-glucose, sodium chloride, sodium hydroxide, hexokinase (HK) from yeast, glucose 6-phosphate dehydrogenase from *Zymomonas mobilis* (G6PDH) and guanidine hydrochloride were obtained from Wako Pure Chemical Industries, Ltd. (Osaka, Japan). D-Glucose-6-phosphate disodium salt hydrate (G6P) was obtained from Combi-Blocks, Inc. (San Diego, USA). Poly-L-lysine hydrobromide (PLL; molecular weight of 4,000–15,000) was obtained from Sigma-Aldrich Co. (St Louis, MO, USA). Rhodamine B isothiocyanate (RBITC) was obtained from Santa Cruz Biotechnology, Inc. (California, USA). Fluorescein-4-isothiocyanate (FITC) and 3-[4-(2-Hydroxyethyl)-1-piperazinyl] propanesulfonic acid (EPPS) were obtained from Dojindo (Kumamoto, Japan).

Precipitation rate of nucleotides, PLL and enzymes

The formation of the liquid droplets of nucleotides with PLL was investigated by precipitation rate of the nucleotides. Concentration dependence of PLL for the liquid droplet formation was measured as follows. The PLL stock solution was prepared with 0–10 mM PLL (monomer concentration) in 10 mM HEPES buffer (pH 7.0). Aliquots of 100 μL of various nucleotide solutions containing 1 mM nucleotide in 10 mM HEPES buffer (pH 7.0) were mixed with 100 μL of the PLL stock solution. Samples were then centrifuged at 18,000 g for 20 min at 25°C. The concentrations of nucleotide in supernatant were determined from absorbance at 260 nm using a ND-1000 spectrophotometer (NanoDrop Technologies, Wilmington, DE). Precipitation rates were calculated as

$$\text{Precipitation rate (\%)} = [1\text{-}C_0(\text{mM})/C_n(\text{mM})] \times 100(\%)$$

where C_0 is the nucleotide concentration in the supernatant without PLL and C_n is the nucleotide concentration in the supernatant with PLL.

The concentration of PLL, ATP, and NADP in the mixture was determined based on the peak area in the HPLC chromatograms. Aliquots (100 μL) of 2.5 mM PLL (monomer concentration), 0.5 mM ATP or 0.5 mM NADPH in 10 mM HEPES (pH = 7.0) were centrifuged at 18,000 g for 20 min at 25 °C, and their supernatant was analyzed by HPLC. HPLC chromatograms were recorded using an LC-20A system (pump LC-20AD, diode array detector SPD-M20A; Shimadzu Corporation, Kyoto, Japan) equipped with a C18 column (Phenomenex binetex 5.0 μm 250 × 4.6 mm; Phenomenex Inc., Torrance, CA, USA). The analytical HPLC of PLL was conducted with an isocratic elution of 10 mM HEPES buffer (pH = 7.0) at 1 mL min^{-1} at 25 °C. The analytical HPLC of nucleotides (ATP and NADP) was performed with mobile phase A [10 mM HEPES (pH = 7.0) with 1000 mM NaCl] and B [10 mM HEPES (pH = 7.0)] at 1 mL min^{-1} at 25 °C using the following stepwise isocratic elution: 20%B (0–2 min), 15%B (2–4min), and 0%B (4–15 min). PLL and nucleotides were monitored at 200 nm and 260 nm, respectively.

The concentration of HK-F and G6PDH-RB in the mixture was determined based on the fluorescence intensity. Calibration curves were created based on the fluorescence intensity of aliquots (300 μL) of 0-0.1 unit/mL HK-F or G6PDH-RB, 0.5 mM ATP, 0.5 mM NADP, 1 mM $MgCl_2$ in 10 mM HEPES (pH = 7.0) using a Varioskan LUX microplate reader (Thermo Fisher Scientific, Waltham, US). Subsequently, aliquots (600 μL) of 2.5 mM PLL (monomer concentration), 0.1 unit/mL HK-F and G6PDH-RB, 0.5 mM ATP, 0.5 mM NADP, 1 mM $MgCl_2$ in 10 mM HEPES (pH = 7.0) were centrifuged at 18,000 *g* for 20 min at 25 °C, before the enzyme concentration was determined based on the fluorescence intensity of the supernatant according to the calibration curves.

Fluorescence labeling of HK and G6PDH

Enzymes labeled with amine-reactive dyes were prepared using manufacturer's instructions after slight modification. HK and G6PDH were labeled with FITC (ex/em: 495/520) and RBITC (ex/em: 555/580), respectively. A solution of FITC (1.77 mM) or RBITC (1.77 mM) in DMSO (50 μL) was quickly added to a stirred solution of HK (17.7 μM) or G6PDH (17.7 μM) in 20 mM EPPS (950 μL) (pH = 8.5) at room temperature. After the reaction mixture was gently stirred for 1.5 h at room temperature, and 200 mM Tris-HCl (100 μL) (pH = 8.5) was added. The enzyme-dye conjugates were purified by filtering using Amicon Ultra-0.5 mL centrifugal filters, molecular weight cutoff (MWCO) of 30 kDa (Millipore Sigma). The final concentration of each enzyme was determined with a bicinchoninic acid (BCA) assay. The number of FITC and G6PDH conjugated to each enzyme was determined from absorbance at 495 nm (Abs495) and 556 nm (Abs556) of the enzymes in 10 mM HEPES (pH = 7.0), respectively. using the equations [FITC] = (Abs495/75800) and [RBITC] = (Abs556/87000). The number of dye molecules per HK or G6PDH enzyme molecule was 0.55 and 0.41, respectively. HK-RBITC and G6PDH-FITC were also prepared using the same procedure, where the number of dye molecules per HK or G6PDH enzyme molecule was 0.14 and 0.26, respectively.

Enzymatic reaction assays for HK and G6PDH

The concentration of HK and G6PDH was determined from absorbance at 280 nm by using an ND-1000 spectrophotometer (NanoDrop Technologies, Wilmington, DE) with extinction coefficients of 46090 $M^{-1}cm^{-1}$ and

67505 $M^{-1}cm^{-1}$. Each enzymatic reaction was measured with a solution of the following final composition:

1) Reaction of HK: 2 mM D-glucose, 0.5 mM ATP, 1 mM $MgCl_2$, 0.64 μg/mL (0.1 unit/mL) HK, 0-5 mM PLL (monomer concentration) in 10 mM HEPES (pH = 7.0).

2) Reaction of G6PDH: 2 mM G6P, 0.5 mM NAD or NADP, 0.38 μg/mL (0.1 unit/mL) G6PDH, and 0-5 mM PLL (monomer concentration) in 10 mM HEPES.

3) Sequential reaction of HK and G6PDH: 2 mM D-glucose, 0.5 mM ATP 0.5 mM NAD or NADP, 1 mM $MgCl_2$, 0.64 μg/mL (0.1 unit/mL) HK, 0.38 μg/mL (0.1 unit/mL) G6PDH, and 0-5 mM PLL (monomer concentration) in 10 mM HEPES (pH = 7.0).

A sample solution except for the substrate (D-glucose or G6P) was prepared, and 10 minutes later, the reaction was started by the addition of the substrate. After defined periods, the reaction was stopped by the addition of an equal volume of 6 M guanidine hydrochloride. Substrate and products (ATP, ADP, NADP, NADPH) were separated, and their concentrations were quantified using an HPLC system under the same conditions as for the PLL/ATP/NADP solution supernatant concentration analysis (*vide supra*). In order to estimate the initial enzyme kinetics (v_0), an analysis was performed using a non-linear model that considered the decrease in reaction kinetics due to substrate depletion or product inhibition.[1]

Optical and fluorescence microscopy

All images were recorded on an all-in-one fluorescence microscope BZ-X710 (KEYENCE, Osaka, Japan). Phase-contrast microscopy images using mixtures of PLL and nucleotides (Figure 1) were taken as follows. The PLL stock solution was prepared with 0–10 mM PLL (monomer concentration) in a 10 mM HEPES buffer (pH = 7.0). Aliquots of 50 μL of various nucleotide solutions containing 1 mM nucleotide in a 10 mM HEPES buffer (pH = 7.0) were mixed with 50 μL of the PLL stock solution. Samples of 100 μL were plated in ultra-low attachment 96 well plates (Coaster, Corning). The images (Figure 1) were taken 5 hours after mixing the solutions.

Phase-contrast and fluorescence images showing droplet formation and molecular localization during the enzymatic reaction were taken as described below. Sample and substrate solutions were prepared for the reaction with HK and G6PDH, and for continuous reaction with both HK and G6PDH, respectively. For the HK reaction (Fig. 2B), the sample solution was 10 mM HEPES, 0.5 mM ATP, 1 mM MgCl2, 0.64 μg/mL (0.1 units/mL) HK-F, and 0–5 mM PLL (monomer concentration) (pH = 7.0) (90 μL). The substrate solution was 10 mM HEPES, 20 mM D-glucose (10 μL). For G6PDH (Fig. 3B), the sample solution was 10 mM HEPES, 0.5 mM NADP or NAD, 1 mM $MgCl_2$, 0.38 μg/mL (0.1 unit/mL) G6PDH-RB, and 0–5 mM PLL (monomer concentration) (pH = 7.0) (90 μL). The substrate solution was 10 mM HEPES, 20 mM G6P (10 μL). For the sequential reaction, the sample solution was 10 mM HEPES, 0.5 mM ATP; 0.5 mM NADP or NAD, 1 mM $MgCl_2$, 0.64 μg/mL (0.1 units/mL) HK-F, 0.38 μg/mL (0.1 units/mL) G6PDH -RB, and 0–5 mM PLL solution (monomer concentration) (pH = 7.0) (90 μL). The substrate solution was 10 mM HEPES, 20 mM D-glucose (10 μL). Each sample solution (90 μL) was placed in ultra-low-attachment 96 well plates (Coaster, Corning) and allowed to stand for 5 hours at room temperature, before the substrate solution (10 μL) was added to start the reaction. Time-lapse images were recorded every minute during the enzymatic reaction. NADPH, HK-F, and G6PDH-RB were excited at 360 nm, 470 nm, or 545 nm, respectively, and the corresponding emissions were detected at 460 nm, 525 nm, or 605 nm, respectively.

Image processing and statistical analysis

The droplet areas were determined using the ‘‘Analyze Particles’’ function (smallest detected size was set to 1 μm^2, circularity 0.5 – 1) using image processing software (Image J, National Institutes of Health), in which the

fluorescence images after threshold processing were used. Statistical significance was evaluated with two-tailed homoscedastic Student's *t*-test using Microsoft Excel.

Section 2. Table and Figures

Table S1 Precipitation rate of fluorescent labelled enzyme (%) in the ATP/PLL or NADPH/PLL droplets.

	ATP/PLL	NADPH/PLL
HK-F	57.7 ± 1.2	56.8 ± 3.8
G6PDH-RB	45.8 ± 1.4	61.4 ± 2.3

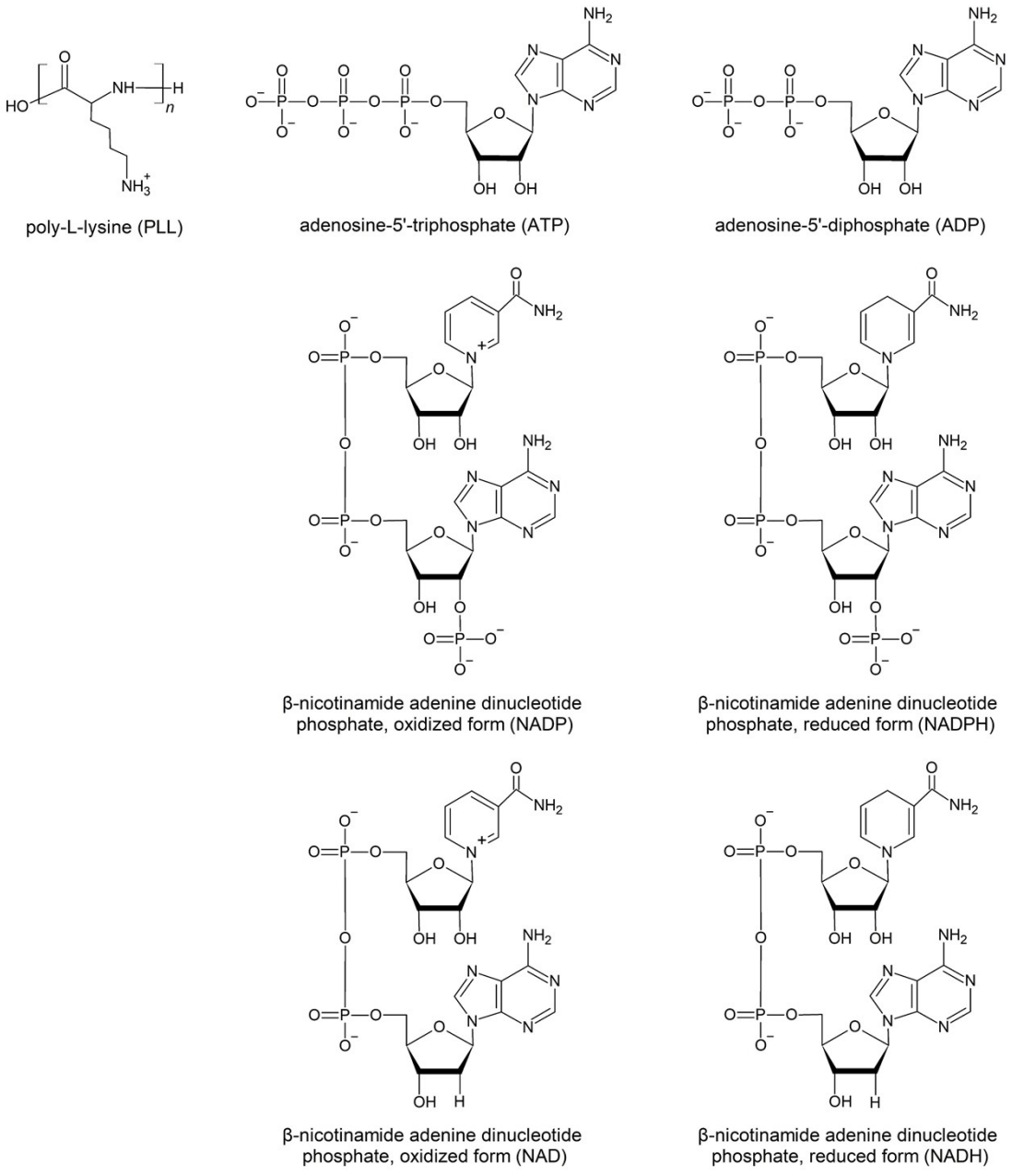

Figure S1. Chemical structures of poly-L-lysine and nucleotides.

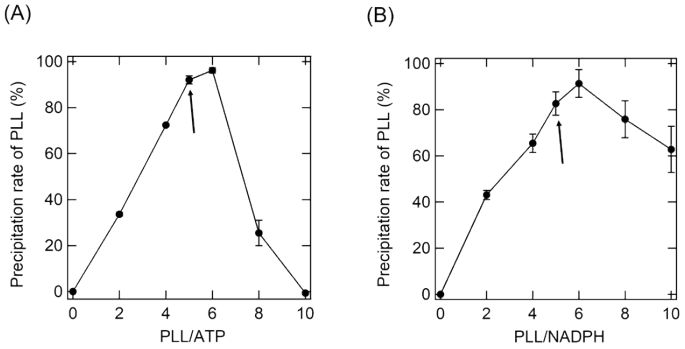

Figure S2. Precipitation rate (%) of PLL in the presence of ATP (A) or NADPH (B). All solutions were prepared with 0.5 mM nucleotides, PLL concentrations between 0–5 mM (monomer concentration), and 10 mM HEPES (pH = 7.0). The arrows indicate the condition under which the microscopy images were recorded in Figs. 2-4.

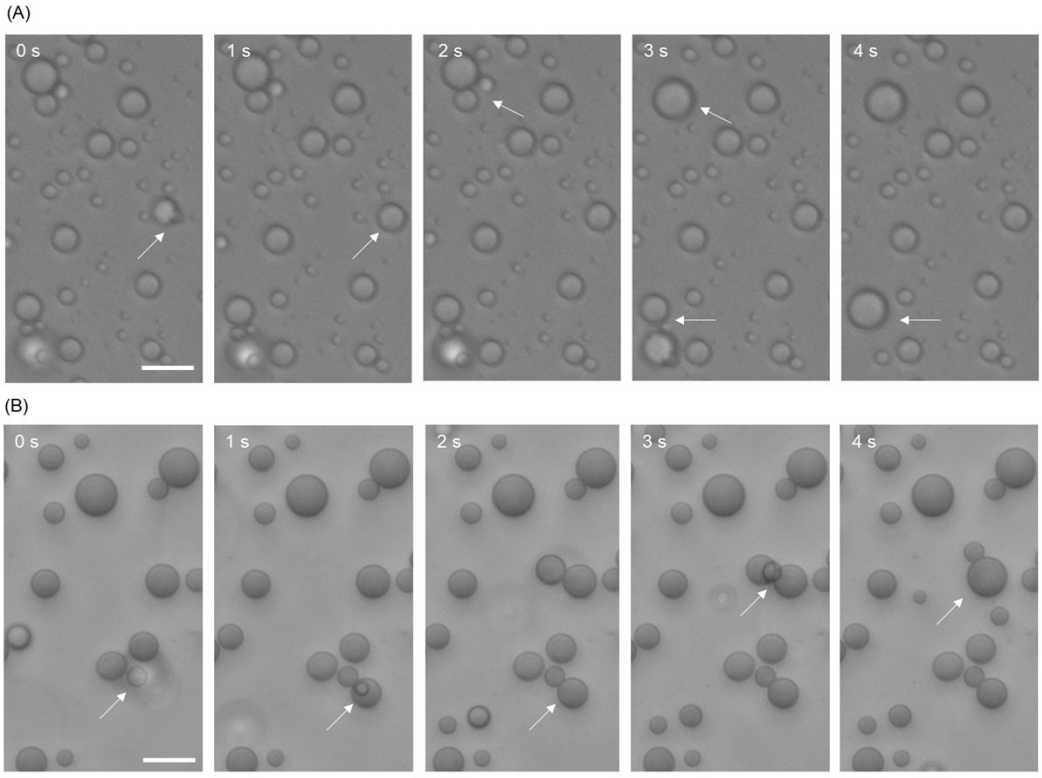

Figure S3. Coalescence process of the ATP/PLL droplets (A) and NADPH/PLL droplets (B). Arrows indicate droplets where fusion has occurred, which is one of the criteria for indicating that the assemblies are liquid droplets with high fluidity.[2,3] All solutions were prepared with 0.5 mM nucleotides, 2.5 mM PLL (monomer concentration), and 10 mM HEPES (pH = 7.0); scale bar: 10 μm.

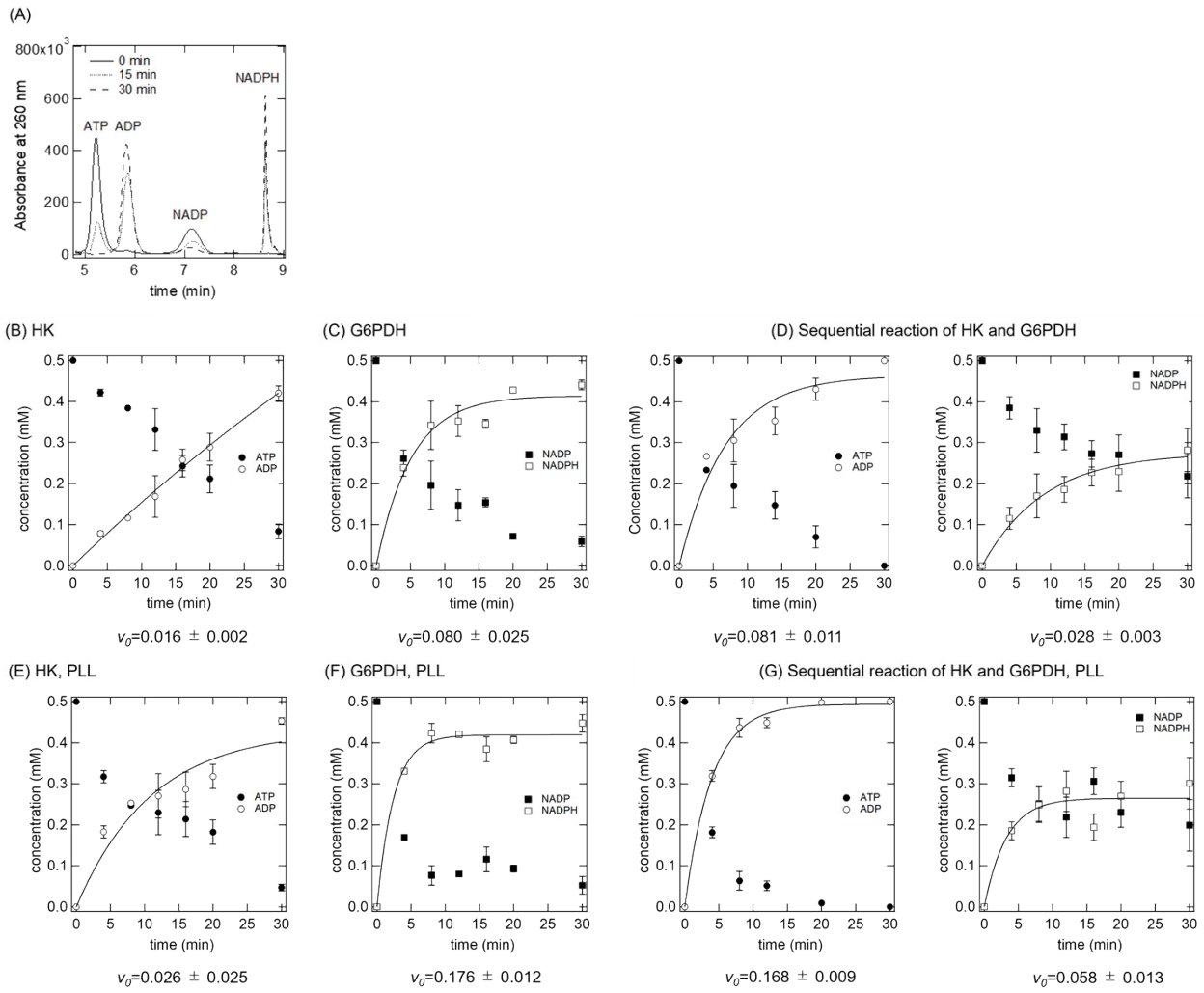

Figure S4. Time course of the concentrations of each nucleotide in the enzyme reaction. (A) Typical HPLC chromatogram. Enzyme reaction in the absence of PLL (B-D) and presence of PLL (E-G); (B, E) HK reaction, (C, F) G6PDH reaction, and (D, G) the glycolytic sequential reaction. Closed circles: Substrates (ATP or NADP); closed squares: Products (ADP or NADP). Data are shown as mean values ± standard deviation (n = 5). Changes in product concentrations (ADP or NADPH) were fitted by a nonlinear kinetic time course model. [1] The solution conditions were the same as those in Fig. 2 (for B and E), Fig. 3 (for C and F), and Fig. 4 (for D and G).

127

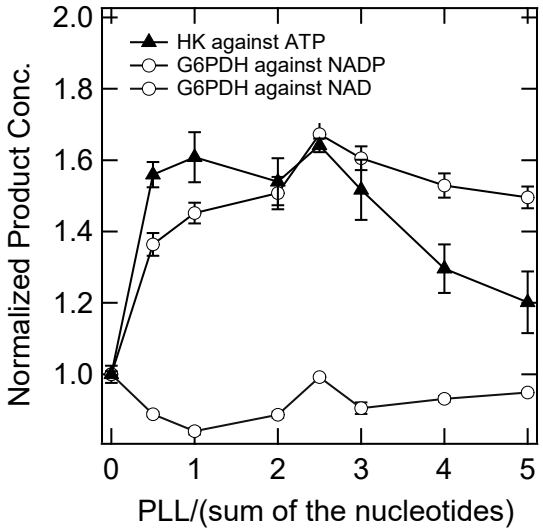

Figure S5. The concentrations of nucleotides produced by each enzymatic reaction in the presence of various concentrations of PLL. All solutions were prepared with 0.5 mM nucleotides, PLL concentrations between 0–5 mM (concentration refers to the monomer unit), and 10 mM HEPES (pH = 7.0). Each result of enzyme activity was defined by the slope of the product concentration over 0-10 minutes, and normalized by the activity without the addition of PLL.

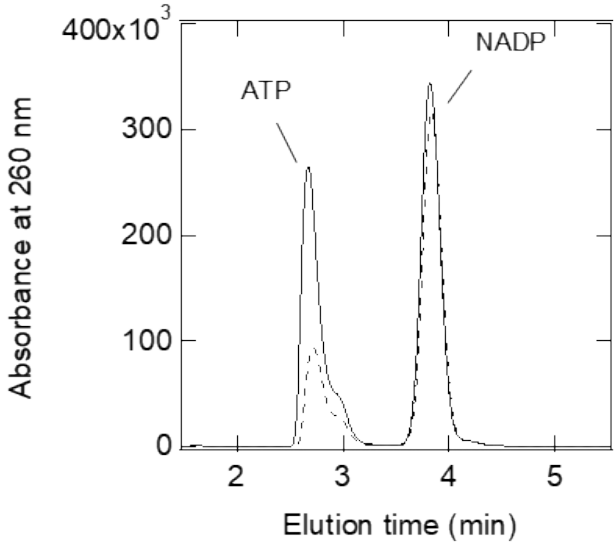

Figure S6. The concentration of ATP and NADP in the supernatant in the PLL/ATP/NADP system. The solution containing 0.5 mM ATP, 0.5 mM NADP in 10 mM HEPES (pH = 7.0) in the presence or absence of 2.5 mM PLL (concentration refers to the monomer unit) was analyzed with HPLC. From the area ratio of the region corresponding to each nucleotide in the solid line (without PLL) and the broken line (with PLL), it was calculated that 60.79±0.39 % and 8.90±1.07 % of ATP and NADP precipitated upon the addition of PLL, respectively.

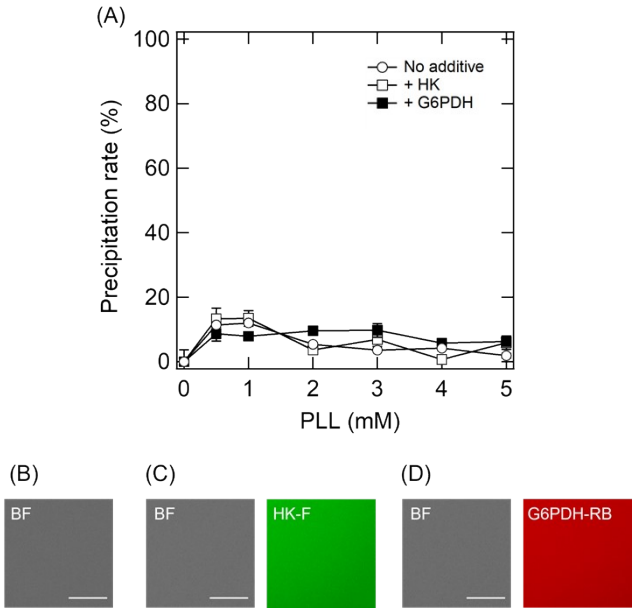

Figure S7. The addition of the labelled enzymes did not induce the formation of PLL/NADP droplets. (A) The NADP precipitation rate upon addition of PLL in the absence or presence of the labelled enzymes. 0.5 mM NADP was mixed with 0-5 mM PLL (concentration refers to the monomer unit) in 10 mM HEPES (pH = 7.0) in the absence (○) and the presence of 0.1 unit/mL HK (□) or 0.1 unit/mL G6PDH (■). (B-D) Optical microscopy images of the solutions containing NADP and PLL in the absence or presence of the labelled enzymes. A mixture of 0.5 mM NADP and 2.5 mM PLL (B); 0.5 mM NADP, 2.5 mM PLL, and 0.1 unit/mL HK-FITC (C); 0.5 mM NADP, 2.5 mM PLL and 0.1 unit/mL G6PDH-RB (D); scale bar: 10 μm. Even in the presence of the labelled enzymes, no PLL/NADP droplets were formed under the conditions of the enzyme sequential reaction shown in Fig. 4. This result supports the hypothesis that the droplets observed before the reaction ('Pre' in Fig. 4B) were mostly PLL/ATP droplets.

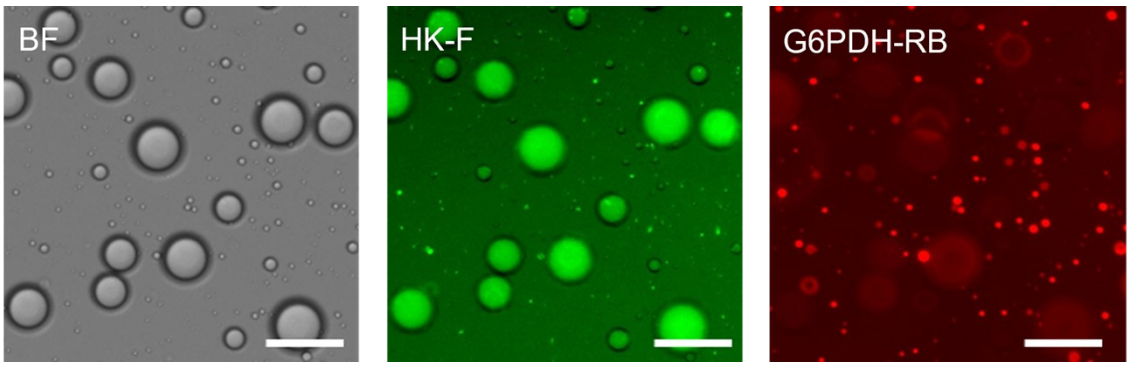

Figure S8. Coexistence of different droplets that selectively incorporate the labelled enzymes. The experimental conditions were the same as those for 'Pre' in Fig. 4B, i.e., before the addition of substrate D-glucose; scale bar: 20 μm. Based on the images, it was confirmed that the large green droplets, which contain HK-F, and that the small red droplets, which contain G6PDH-RB, were present independently. It should also be noted that the large HK-F-rich droplets also contained a small amount of G6PDH-RB.

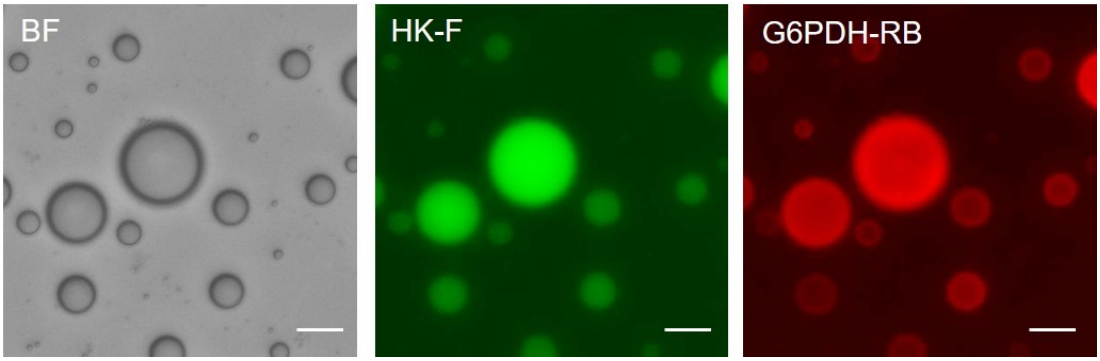

Figure S9. Droplets that selectively incorporate different enzymes are in a kinetically trapped state. The experimental conditions were the same as those for 'Pre' in Fig. 4B, i.e., before the addition of substrate D-glucose. The solution was prepared and incudated for 5 hours, before the solution was stirred by pipetting before the microscopy images were recorded after another 5 hours of incubation; scale bar: 20 μm. In contrast to the results shown in Figs. 4 and S8, both HK-F and G6PDH-RB were incorporated in almost all droplets, suggesting that droplets with heterogeneous compositions are in a nonequilibrium or kinetically trapped state.

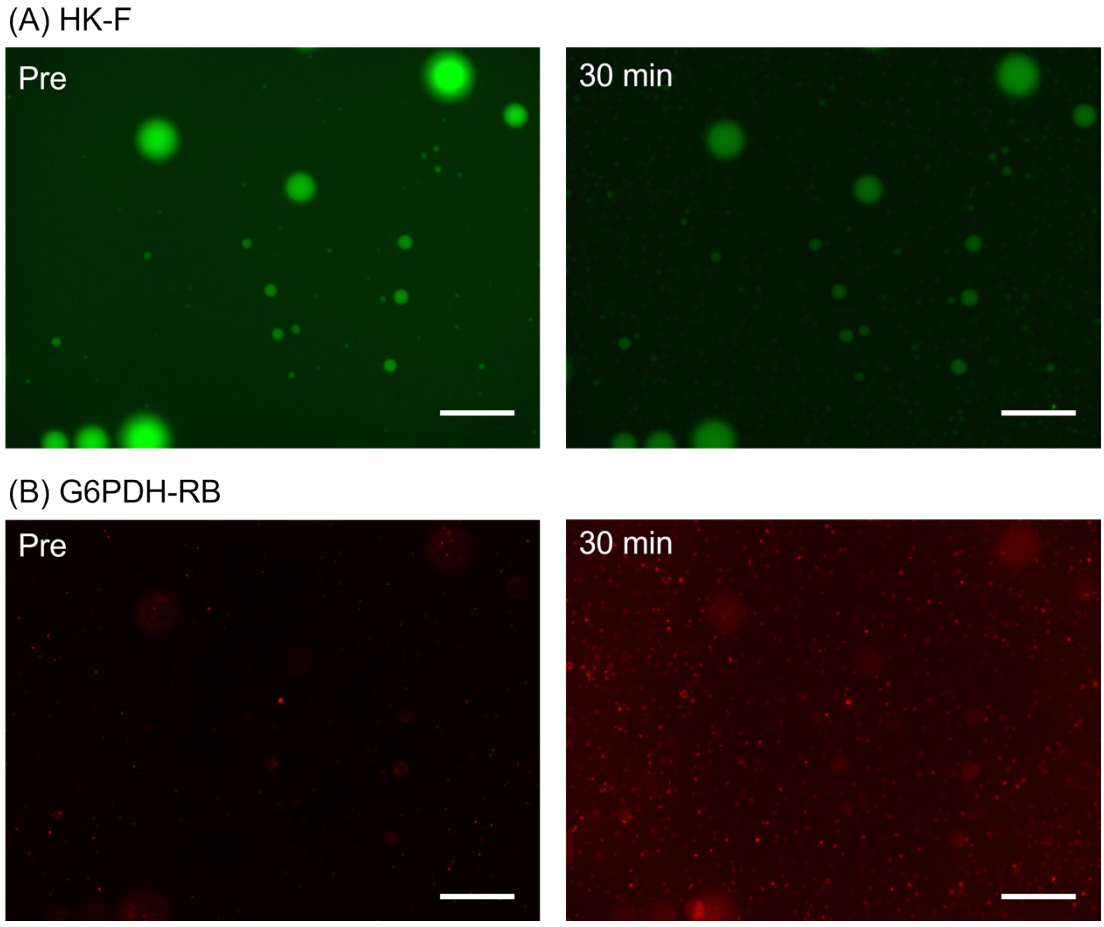

Figure S10. Changes in droplets before (Pre) and after (30 min) the sequential enzymatic reaction (wide-field view). The localization of (A) HK-F and (B) G6PDH-RB is shown; scale bar: 50 μm.

143

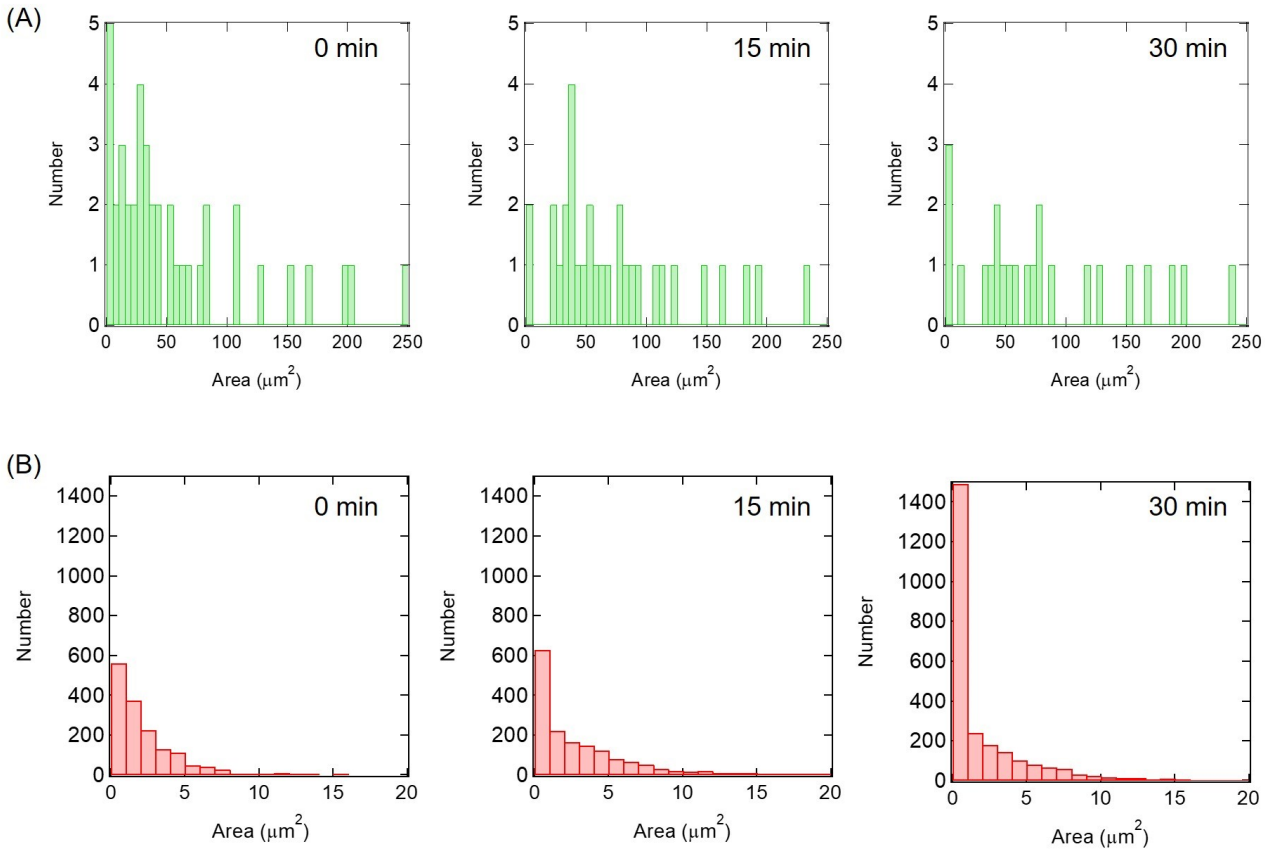

Figure S11. Histograms for the area of droplets that contain different labelled enzymes. Under the same experimental conditions as those for Fig. 4B, the areas of green droplets that contain HK-F (A) and those of the red droplets that contain G6PDH-RB (B) were counted in the fluorecence microscopy images before (0 min), during (15 min), and after (30 min) the enzyme reaction. The histograms show that particularly small HK-F-containing dropelts (<50 μm^2) disappeared preferentially. For droplets containing G6PDH-RB, especially the smaller ones (<1 μm^2) markedly increased. The disappearance observed in the small green droplets was presumably because ATP was consumed before NADPH was supplied to the small droplets. The occurrence observed in small droplets suggests that excess G6PDH-RB was preferentially incorporated into newly generated PLL/NADPH droplets.

144

145

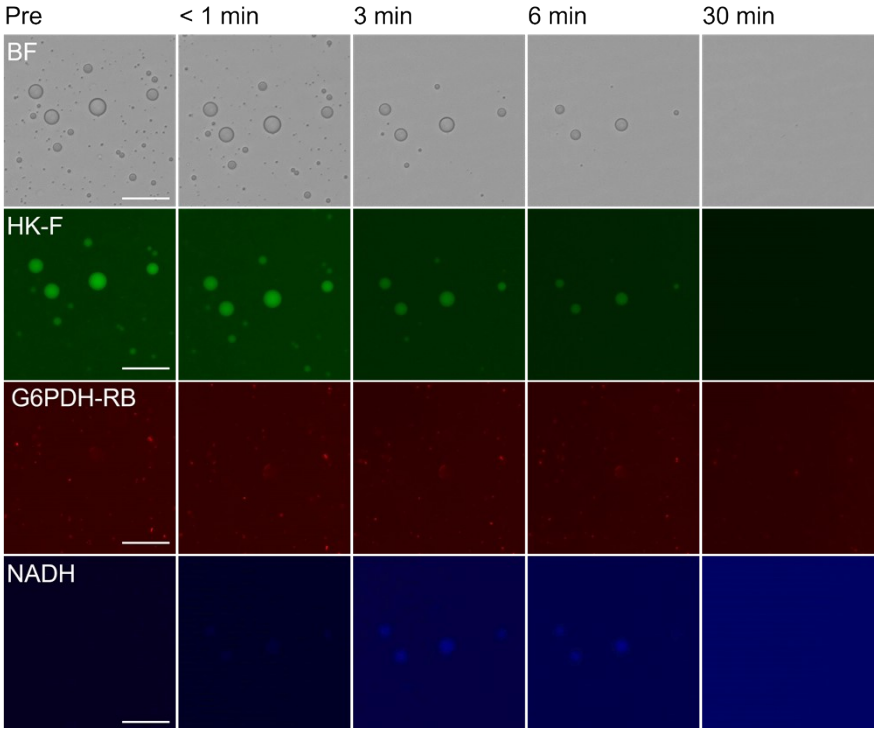

Figure S12. Microscopy images of droplet changes accompanied with the sequential enzymatic reactions using NAD instead of NADP as a substrate. The solution conditions were the same as those in Fig. 4; scale bar: 20 μm.

146
147

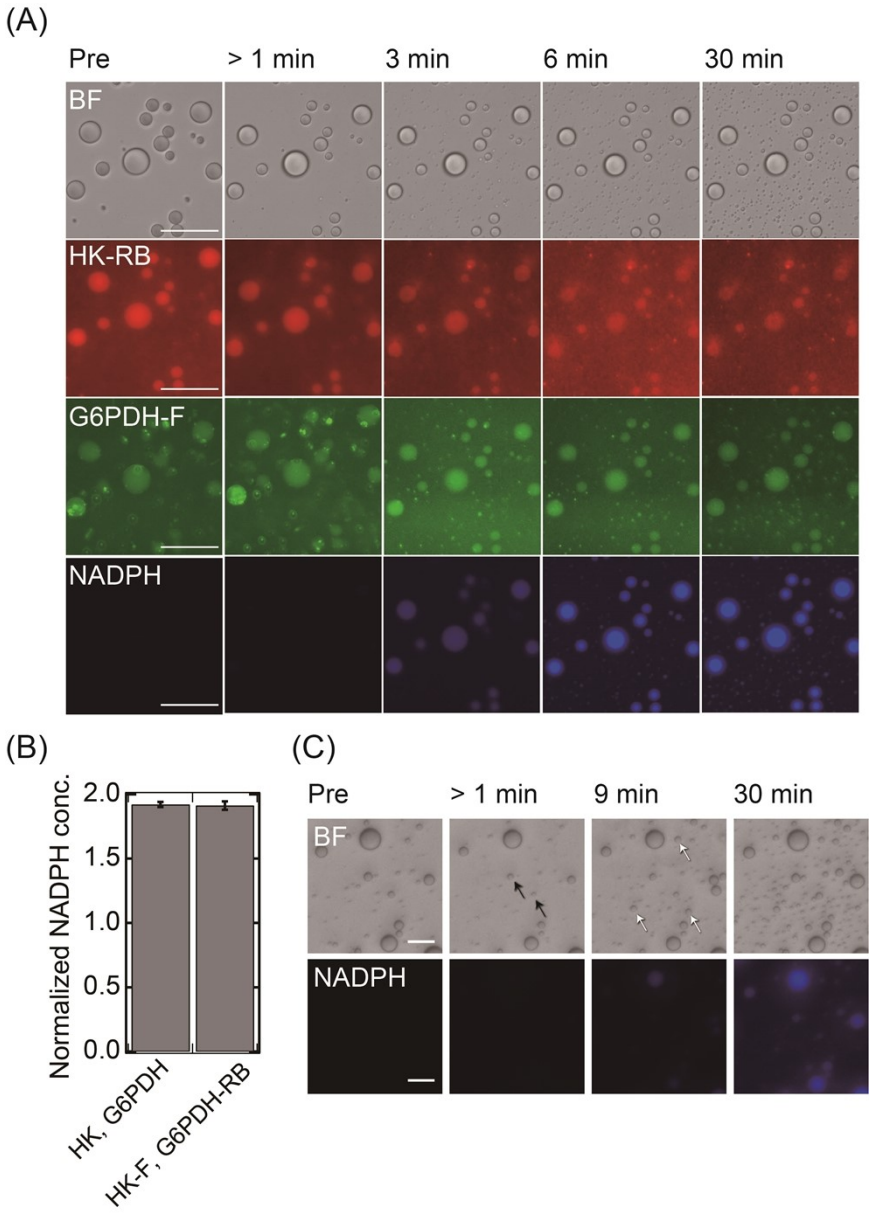

Figure S13. Effect of enzyme labeling on the dynamic droplet behavior and the enzyme activity. (A) Microscopy images of the droplet changes accompanied by the sequential reaction when the fluorescent molecules for labelling were replaced. The experimental conditions were the same as those in Fig. 4B, except that HK-RB and G6PDH-K were used instead of HK-F and G6PDH-RB; scale bar: 20 μm. When the reaction was initiated by the addition of D-glucose, the HK-RB-rich droplets became smaller and their brightness decreased, while simultaneously, new G6PDH-K-rich droplets were formed and grew. In addition, with the passage of time, NADPH-containing droplets were localized not only in newly formed droplets but also in the original droplets. This behavior is similar to that observed in Fig. 4B. (B) The effect of labeling on the concentration of the final product of the enzyme sequential reaction. Labelled and unlabeled enzymes were used to quantify the concentration of NADPH at 10 min after the initiation of the enzyme sequential reaction under the same experimental conditions as those in Fig. 4D. The result showed that the concentration of NADPH was almost the same with or without labeling. (C) Microscopy images of droplet changes accompanied by the sequential reaction when non-labelled HK and G6PDH were used. The sample conditions were the same as those in Fig. 4B, except that the non-labeled enzymes were used. Black and white arrows show the partially dissolved droplets and the newly formed droplets, respectively. Similar behavior was observed in Figs. 4B and S13A. Taken together, these results suggest that enzyme labeling has no significant effect on the sequence of processes involving dynamic changes in the droplets.

148

Section 3. Effect of enzymes and substrates on droplets

In order to understand the relationship between the progress of the enzymatic reactions and the dynamic changes of the droplets, it is desirable to clarify how the addition of molecules other than nucleotides (ATP and NADPH) and PLL, which are essential for droplet formation, such as substrate sugars (D-glucose and G6P) and labeled enzymes (HK-F and G6PDH-RB) affect droplet formation. Therefore, we observed the effects of the labeled enzymes and the substrate sugars on nucleotide/PLL droplet formation. In the ATP/PLL system (Fig. 2), even though the concentration of HK-F at 0.64 μg/mL (0.1 units/mL) was very low, larger droplets were observed at 4 hours after mixing (Fig. S14A), while 2 mM D-glucose did not affect the formation of droplets (Fig. S14B). Considering the extent of the area where droplets are not present, changes in the interfacial tension of the droplets due to the enzyme encapsulation might cause an increase in growth rate of the droplets due to Ostwald ripening.[4] In the NADP/PLL system (Fig. 3), no PLL/NADP droplets were formed with or without the use of both 0.38 μg/mL (0.1 units/mL) G6PDH-RB and 2 mM G6P (Fig. S15). In the PLL/ATP/NADP system (Fig. 4), 2 mM glucose did not affect droplet formation (Figs. S16A and S16B). Interestingly, both HK-F (0.64 μg/mL) and G6PDH-RB (0.38 μg/mL) increased the droplet size, while the incorporation of the enzymes into the droplets differed. In other words, HK-F was incorporated independent of the droplet size, while G6PDH-RB was incorporated predominantly into smaller droplets (Figs. S16C and S16D). Comparable differences in droplet size dependence of enzyme uptake were also observed in the presence of both enzymes (Fig. S16F), similar to the results shown Fig. 4B. The reason for this behavior is still unclear; unexpectedly, in the absence of HK-F and in the presence of G6PDH-RB and glucose, G6PDH-RB was incorporated into the droplets more than in the absence of glucose (Fig. S16E). These results suggest that the growth rate of the droplets varies with the presence or absence of enzymes, and that the presence of sugars had little effect except in a limited number of cases. It should be noted that the addition of the enzymes affects the droplet-fusion process, but not the droplet formation/non-formation. Even with these fusion-promoting effects, it should be clear that incorporation into the droplets accelerates the enzymatic reaction and that the enzymatic reaction is coupled to the dynamic behavior of the droplets.

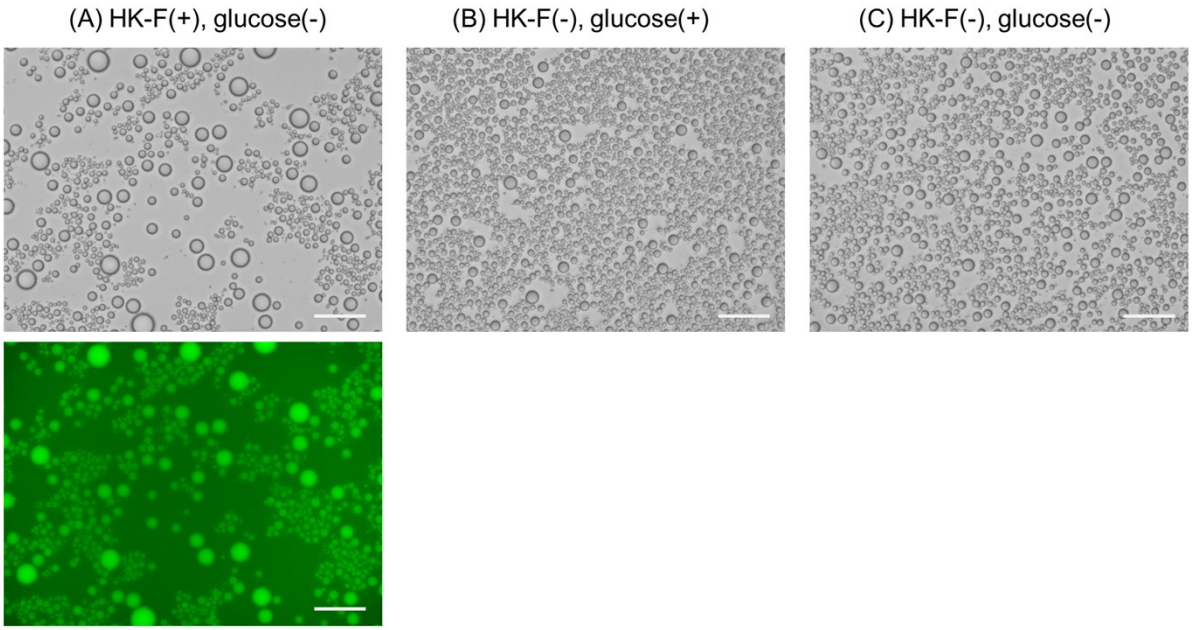

Figure S14. The effect of HK-F and D-glucose on the ATP/PLL droplets. (A) With HK-F and without D-glucose, (B) without HK-F and with D-glucose, and (C) without HK-F and D-glucose. The solutions contained 0.5 mM ATP, 2.5 mM PLL (concentration refers to the monomer unit), 0 or 0.64 μg/mL HK-F, 0 or 2 mM D-glucose, and 10 mM HEPES (pH = 7.0); scale bar: 50 μm.

174

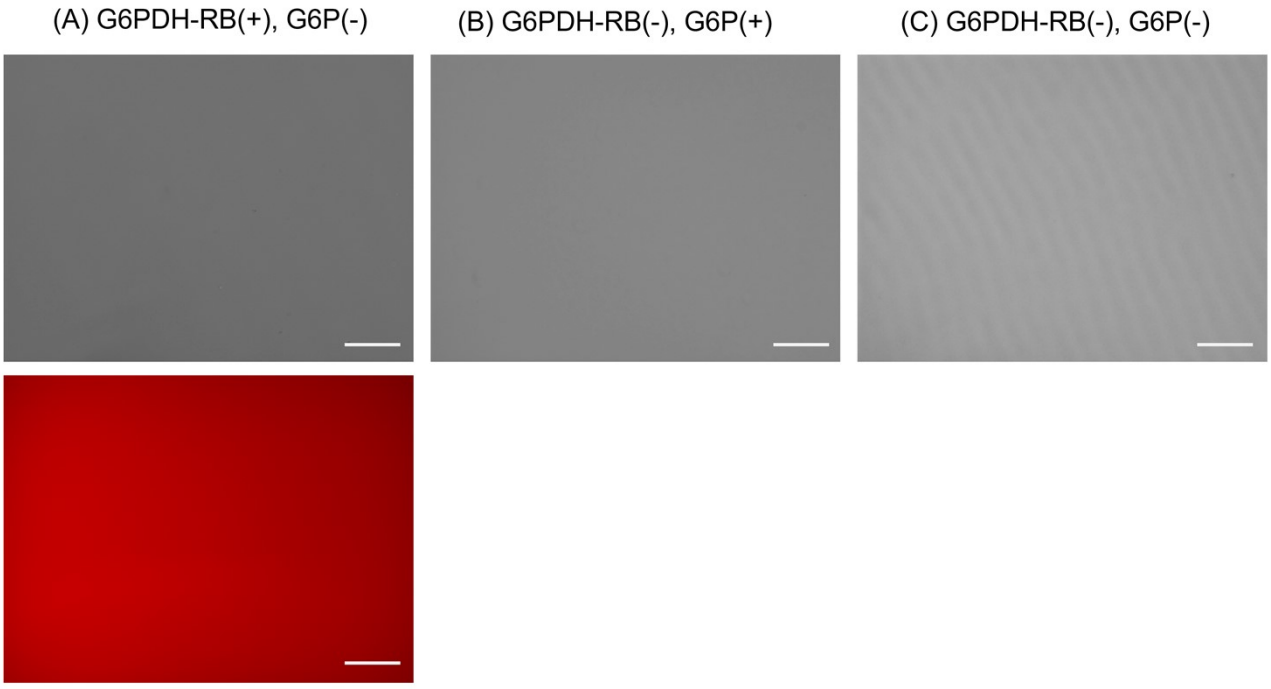

Figure S15. The effect of the G6PDH-RB and G6P on the formation of NADP/PLL droplets. (A) With G6PDH-RB and without G6P, (B) Without G6PDH-RB and with G6P, and (C) without both G6PDH-RB and G6P. The solutions contained 0.5 mM NADP, 2.5 mM PLL (concentration refers to the monomer unit), 0 or 0.38 μg/mL G6PDH-RB, 0 or 2 mM G6P, and 10 mM HEPES (pH = 7.0); scale bar: 50 μm.

175

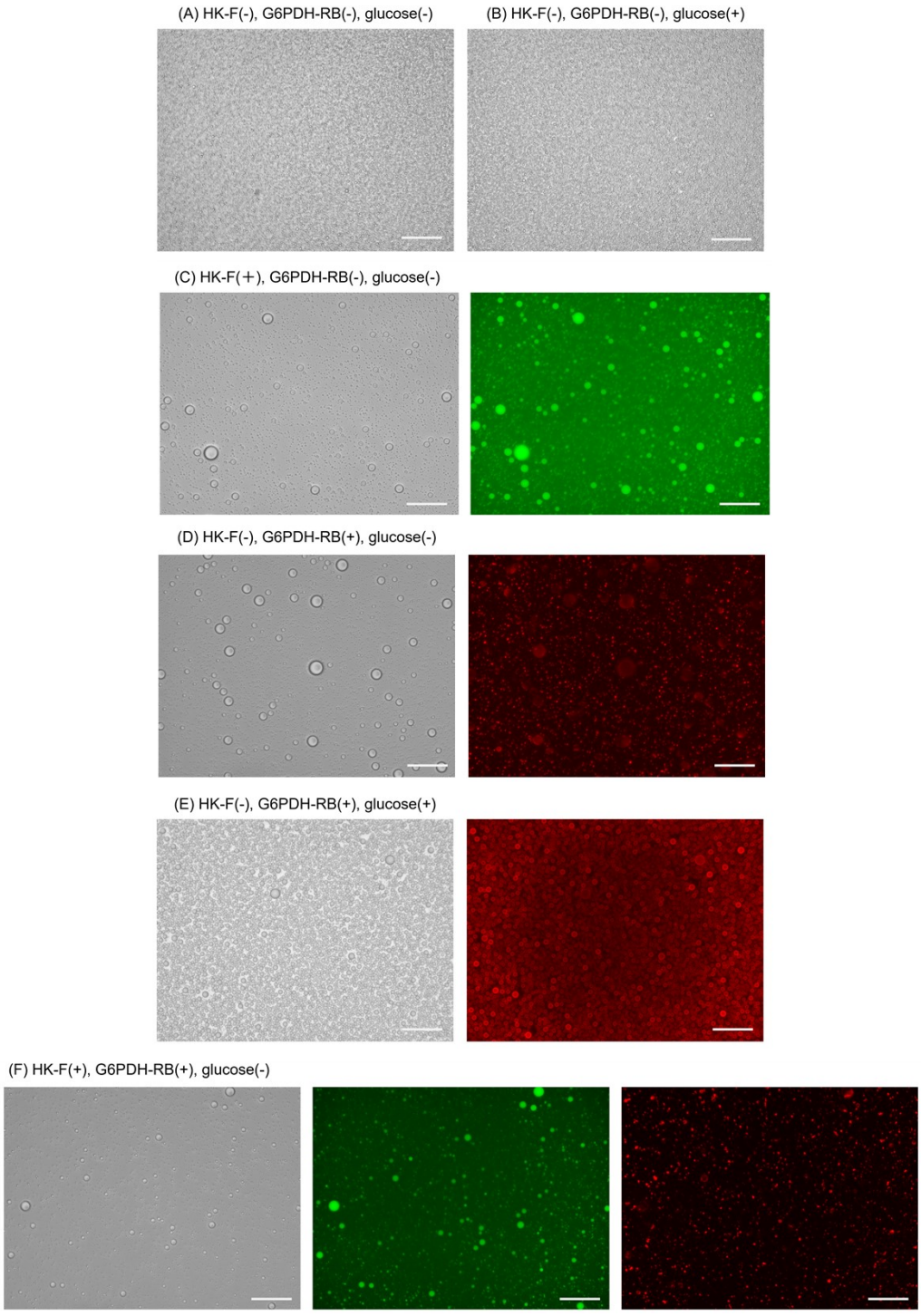

Figure S16. The effect of the HK-F, G6PDH-RB, and D-glucose on the ATP/NADP/PLL droplets. (A) No addition, (B) with D-glucose, (C) with HK-F, (d) with G6PDH-RB, (e) with G6PDH-RB and D-glucose, (f) with HK-F and G6PDH. The solutions contained 0.5 mM ATP, 0.5 mM NADP, 2.5 mM PLL (concentration refers to the monomer unit), 0 or 0.64 μg/mL HK-F, 0 or 0.38 μg/mL G6PDH-RB, 0 or 2 mM D-glucose and 10 mM HEPES (pH = 7.0); scale bar: 50 μm.

176

Section 4. Legends for Supplementary Movies

Movie S1. Microscopy images of droplet changes accompanied by the sequential reaction; scale bar: 50 μm. The experimental conditions were the same as those in Fig. 4B.

Movie S2. The change of localization of HK-F under the conditions of Movie S1; scale bar: 50 μm.

Movie S3. The change of localization of G6PDH-RB under the conditions of Movie S1; scale bar: 50 μm.

Movie S4. The production and localization of NADPH under the conditions of Movie S1; scale bar: 50 μm.

Section 5. References

1 W. Cao and E. M. De La Cruz, *Sci. Rep.*, 2013, **3**, 3–7.

2 C. P. Brangwynne, C. R. Eckmann, D. S. Courson, A. Rybarska, C. Hoege, J. Gharakhani, F. Jülicher and A. A. Hyman, *Science* **2009**, 324, 1729–1732.

3 H. Zhou, Z. Song, S. Zhong, L. Zuo, Z. Qi, L. Qu, and L. Lai, *Angew. Chem., Int. Ed.* **2019**, 58, 4858–4862.

4 P. W. Voorhees, *Annu. Rev. Mater. Sci.*, 1992, **22**, 197–215.